

13 NOV 1947

MR No. L5J06

1131.3

Carlisle Rm 3513

Copy 1

NATIONAL ADVISORY COMMITTEE FOR AERONAUTICS

# WARTIME REPORT

ORIGINALLY ISSUED  
October 1945 as  
Memorandum Report L5J06

SOME FLIGHT MEASUREMENTS OF PRESSURE DISTRIBUTION

DURING TAIL BUFFETING

By John Boshar

Langley Memorial Aeronautical Laboratory  
Langley Field, Va.

LIBRARY 3191

LANGLEY MEMORIAL AERONAUTICAL  
LABORATORY, BUILDING  
HAMPTON, VIRGINIA

# NACA

WASHINGTON

NACA WARTIME REPORTS are reprints of papers originally issued to provide rapid distribution of advance research results to an authorized group requiring them for the war effort. They were previously held under a security status but are now unclassified. Some of these reports were not technically edited. All have been reproduced without change in order to expedite general distribution.



MR No. L5J06

NATIONAL ADVISORY COMMITTEE FOR AERONAUTICS

MEMORANDUM REPORT

for the

Air Technical Service Command, Army Air Forces  
SOME FLIGHT MEASUREMENTS OF PRESSURE DISTRIBUTION  
DURING TAIL BUFFETING

By John Boshar

SUMMARY

Results are presented of pressure-distribution measurements taken over the horizontal tail surfaces of a Curtiss P-40K airplane during several low-speed pull-ups to abrupt stall in which tail buffeting was experienced.

The results indicate in general that the chordwise load distributions obtained during buffeting are of the type usually associated with angle-of-attack changes. In the early part of the stall the center of buffeting is concentrated on the inboard sections of the tail while after the stall has spread spanwise on the wing the whole tail is enveloped. The average value of the increment in the tail normal-force coefficient due to buffeting was  $\pm 0.25$ . The frequency of the pre-stall disturbances and those after the stall differ; both fluctuations appear regular enough to promote resonant conditions if the tail were of the proper frequency.

INTRODUCTION

One aspect of the buffeting phenomenon about which the designer of the airplane structure has considerable concern is the effect of the magnitude and distribution of the buffet load increment on the design of the horizontal tail surfaces. Although a breakdown of flow over the wing may be experienced at many points of the flight envelope (reference 1), buffeting which occurs at the upper left-hand corner of the V-n diagram has received more attention from the tail loads viewpoint because here

the buffet increment superimposes on an already high quasi-static balance load. Tail load measurements during abrupt stalls at low speeds and accelerations have been reported in reference 2, but the chordwise and spanwise distributions of load which would be aids to the understanding of the mechanics of the buffeting have not been determined.

During an investigation of tail loads being conducted for the Air Technical Service Command on a Curtiss P-40K airplane, some pressure measurements were recorded during low-speed maneuvers in which severe tail buffeting occurred. These maneuvers were incidental to one of the phases of the test program, and not for an investigation of the buffet phenomenon as such; however, the instruments already in the airplane were such that both chordwise and spanwise distributions of the buffeting load increments over the horizontal tail could be determined.

Accordingly, this paper presents the results of both chordwise and spanwise distributions of pressure over the horizontal tail surfaces during two abrupt stalls and isolated pressure measurements at four orifices during two snaprolls.

#### APPARATUS

Airplane.— A three-view line drawing of the Curtiss P-40K airplane used in the tests including a list of some of its geometric characteristics is shown in figure 1. The horizontal tail surfaces of the airplane were equipped with a number of orifices installed opposite each other to measure differential pressures between the upper and lower surfaces.

Pressure-measuring apparatus.— The instrumentation for measuring pressures consisted of manometers which measured the pressure distribution during two of the runs and some special pressure cells which were used to obtain expanded records of pressures at four orifices during the other two runs.

The pressure-distribution measurements were obtained at six spanwise stations on the right side of the tail and at one midspan station on the left side at the orifice locations shown in figure 2. The variation of pressure

with time for each orifice was photographically recorded on a film whose travel was approximately  $1/4$  inch per second. The individual manometer cells are so constructed that they have a volume of approximately 0.3 cubic inch. on the pressure side and about 1.2 cubic inches on the static side. The tubing connecting orifices and cells was of  $5/32$  inch inside diameter and varied in length from 6 to 12 feet so that the volume in the pressure lines varied from 1.7 cubic inches to 3.4 cubic inches. In general, the tubing going to the upper and lower surfaces were of the same length for each orifice.

In the runs during which the expanded pressure records were obtained, the orifices used were chosen on the basis that they were good indices of the loads on the tail surfaces in unstalled maneuvers. These four orifices are shown circled in figure 2. Pressure cells were used which had a film speed travel of  $1\frac{1}{2}$  inches per second, much higher than the speed the pressure-distribution apparatus was capable of. The pressure cells were placed in the tail cone of the fuselage to obtain a minimum of lag and the pressure lines connecting each orifice were balanced.

Miscellaneous instruments.-- During the tests standard NACA instruments were used to record the following quantities against time: the airspeed, elevator and rudder control positions, elevator stick force, normal acceleration, and the angular velocities in pitch, roll, and yaw. A timer was connected into the circuits of all instruments to synchronize the records.

### TESTS

The tests reported herein consisted of four runs performed from power-on steady flight at a pressure altitude of 10,000 feet. Runs 1 and 2 were symmetrical pull-ups to abrupt stalls at indicated speeds of about 140 and 160 miles per hour. Runs 3 and 4 were snaprolls to the right and left, respectively, each at a speed of 135 miles per hour.

## METHOD AND RESULTS

The basic flight data are shown in figure 3 for the symmetrical pull-ups and in figure 4 for the snaprolls.

Symmetrical stalls.- For each of the symmetrical stalls approximately 30 pressure values were read for each of the 75 orifices. The first two lines of figure 5 show, to actual size, typical pressure records obtained from a spanwise line of six orifices located at approximately 30 percent of the chord. Since each trace had a different calibration the relative magnitude of the pressure change at the various points cannot be judged from the figure alone. Also on figure 5 are shown enlargements of a pressure record from each run with circles to identify the points at which the pressures were read. The breaks in the record every 0.1 second permit a more accurate time correlation for such cramped records than would have been possible with an uninterrupted record. Notwithstanding the breaks in the pressure records, during the time period in which the trace lights were on most of the maximum pressure values were recorded as evidenced by the doubling up on the already exposed record shown by the brighter spots at the peaks.

The pressure values on the various orifices on the tail appeared to reach their peaks at the same time. For each of the times corresponding to those of the circled points in figure 5, the chordwise pressure distribution was plotted for the six ribs on the right horizontal tail and the one central rib on the left side. Chordwise pressure distributions for runs 1 and 2 are shown in the isometric views of figures 6 and 7. Because of the width of the record lines, the times at which the peak values occur cannot be determined closer than approximately 0.05 second. The plots therefore represent the maximum and minimum values of pressure distribution occurring in this interval. For each time at which the peaks were read the chordwise pressure distributions were integrated to obtain the rib normal-force coefficient.

Since a continuous variation of normal-force coefficient with time could not be shown because of the timer interruption and cramped record, it seemed advisable to show the maximum and minimum points only and disregard secondary oscillations that were recorded. Further, in order to avoid a confusion of points, the maximum and minimum values for each 0.1-second interval were connected. Shown in this

manner is the variation of the normal-force coefficients on each rib versus time, figure 8, and the variation of the total normal-force coefficient on the right horizontal tail versus time, figure 9. The maximum and minimum values shown by the bars on these figures represent values of  $C_N$ .

Snaprolls.— The variation with time of the differential pressures recorded at four orifices during the snaprolls are shown in figure 10. The traces for these cells are shown without an ordinate scale, since the calibration curves were linear and because only the magnitude of the buffet relative to the mean value is of interest. In the case of figure 10 the calibration factors are approximately the same for all the curves so that the relative pressures can be noted from the deflections.

#### ACCURACY OF RESULTS

The errors which are important to the results presented herein are considered to be those which would effect the distribution of the loads rather than their actual values.

One of the possible causes of error in the distribution is the variability in the amount of resonance magnification experienced by the several orifice-tubing-cell combinations. Figure 11 shows typical curves of the relation between the maximum pressure recorded and the frequency of an impressed sinusoidal pressure for various lengths of tubing (from results of unpublished laboratory tests on various tubing-orifice configurations). Unfortunately, because of differences in the orifice-tubing configurations that were used and the assumption of regular sinusoidal pressure oscillations, the curves of figure 11 can only be used to indicate the possible order of magnitude and the direction of the errors in the recorded pressures. No correction of the data was attempted.

So far as the distributions are concerned, it is believed that for the range of frequencies of the test condition, differences in the amount of resonance for various orifice-tube-cell systems would have reasonably small effect. The source of error in the distributions due to a pressure lag difference for the various tube lengths is negligible since, within the range of lengths used, the differences in length are not great and the tubes have about the same amount of constriction.

The magnification of the total loads may be as high as 25 percent for regular pressure fluctuations. The possible error in total load resulting from reading records, fairing and integrating pressure curves, etc., is estimated to be  $\pm 4$  percent.

## DISCUSSION

In evaluating the distributions and magnitudes of the tail loads in buffeting, it is important to consider the amount of stall experienced by the wing. The buffeting experienced by the tail may range from the desirable mild buffet due to incipient flow separation, which warns of the approach of stall, to the severe shaking associated with the abrupt wing flow breakdown at the maximum lift. A number of items in the flight records of figures 3 and 4 show that the maneuvers were performed in such manner that probably maximum flow breakdown was obtained; namely, the pitching velocity exceeded 1 radian per second, and a very abrupt flow breakdown on the wings is indicated by the sharp drop in the accelerometer records.

The chordwise pressure distributions shown in figures 6 and 7 indicate that during the buffeting the chordwise distributions of pressure are, in general, quite regular and are of the type that would normally be associated with angle-of-attack changes.

Indications of the effect of buffeting on the span load distributions may be obtained from the results shown in figure 8 where it will be noted that immediately after the stall in symmetrical pull-ups the increments in the normal-force coefficients over the inboard ribs are greater than those over the outboard sections. These are shown pictorially in the isometric plots of figures 6 and 7. Later, after the stall develops, the outboard sections also experience high buffet increments, presumably due to an outboard shift of the center of stall at the wing, with the result that the bending moment at the root of the horizontal tail is approximately as great, near the end of run 2, as at the time corresponding to peak acceleration when the tail is already carrying a balancing up load. (A movement of the stall at the wing progressing outboard from the wing root has been noted in tuft studies of an earlier model of this airplane.) Thus, the severity of the buffeting from the structural viewpoint may be governed not only by the

vertical displacement of the tail from the wing as shown in early studies of buffeting but also by the spanwise location of the wing stall relative to the position of the tip of the horizontal tail.

The normal-force coefficients for the right horizontal tail (fig. 9) show that the buffeting causes an increment in normal-force coefficient of approximately  $\pm 0.25$ . It must be remembered that this value of the buffet increment was experienced at low speeds and for high angles of attack.

The pressure records for the snaprolls (fig. 10) indicate that the greater buffeting pressures are experienced on the part of the horizontal tail corresponding to the side on which the wing has stalled. The much higher buffeting increment recorded during run 4 corresponds to a more violent stall as indicated by the more abrupt break in the accelerometer record and the character of the record showing the rolling velocity.

The initial pressure increments of high magnitude shown in figure 10 for orifices CR-3 and DR-3 in run 3 and CL-3 in run 4 presumably are the result of a direct angle-of-attack change caused by the passage of the first shed vortex associated with the flow breakdown at the wing. Similar results are indicated in the records of runs 1 and 2, where it will be noted that the sharp increases in pressure correspond to the sudden break in the accelerometer records.

The extended pressure records of figure 10 are useful in indicating the frequency of the subsequent buffeting. However, since there seems to be no correspondence between the left and right sides during the roll maneuvers the frequency of the wing disturbance would seem to be more accurately noted from pressure records of orifices on the same side of the airplane as that on which the stall occurred.

Reference to the extended pressure records shown in figure 10, in particular for run 4, shows small amplitude pressure fluctuations which occur prior to the stall and whose frequencies differ from those of the buffet after the stall. These suggest the possibility that a tail surface could be set into resonance by the preliminary flow disturbance so that the initial buffet flow would hit a vibrating surface.



Detailed examination of the results given in figures 5 and 10 indicate that, although the fluctuations are irregular in character for any particular orifice, the same fluctuations appear to be experienced simultaneously at all orifices along the semispan even so far as the secondary oscillations are concerned. However, insofar as possible resonance is concerned, the large pressure fluctuations are more important than the smaller ones. The regularity of these changes, as shown in figure 10 by orifices  $C_R-3$  and  $D_R-3$  in run 3 and  $C_L-3$  in run 4, indicate the possibility of resonance with high resulting stresses.

On the basis of the test results presented, little can be said of the wing wake frequency in a general manner. The Strouhal numbers were computed, however, for the two runs for which the frequencies could be determined

(runs 3 and 4). The Strouhal number ( $S = \frac{dF}{V}$ , where  $f$  = wing wake frequency;  $d$ , the dimension of the body perpendicular to the air flow (equal to  $c \sin \alpha$ ); and  $V$ , the flow velocity) has been established as a criterion which connects the frequency of the shed vortices with the velocity. For runs 3 and 4, considering the predominant pressure peaks for the first  $1/2$  second, the frequencies were approximately 15 and 14 cycles per second, respectively. The wing chord at the section from which the disturbance originated was taken to be 7.0 feet and the angle of attack,  $\alpha$  was assumed to be that corresponding to the maximum acceleration. Strouhal numbers of approximately 0.25 and 0.30 were computed for run 3 and run 4, respectively.

Abdrashitov, in a comprehensive survey of the tail buffeting problem (reference 3) reports Strouhal numbers determined in wind tunnel tests of 0.15 for plates and airfoils at high angles of attack. (In a recent paper Krzywoblocki concludes that the Strouhal number is not a constant in general but that it is a constant at high angles of attack, (reference 4).

The evident disagreement between the Strouhal number obtained in the flight tests with those obtained with plain wings tested in wind tunnels is probably to be expected because of differences in the Reynolds numbers, the downstream positions of the points of measurement, and because of the transient character of the flow changes in flight.

## CONCLUSIONS

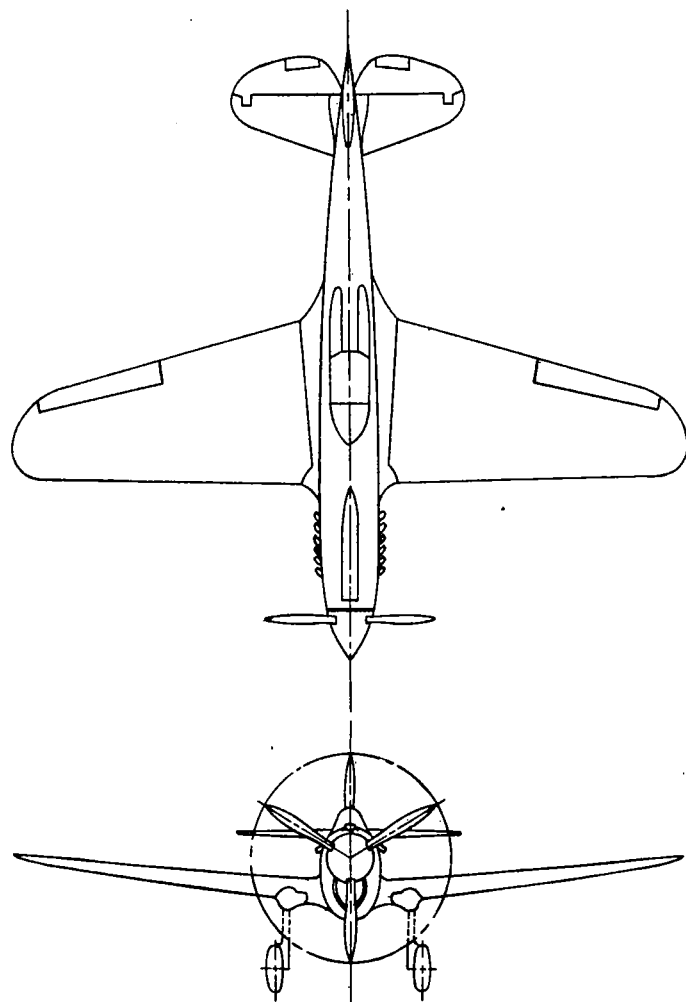
The following conclusions may be drawn from the results:

1. The changes in chordwise pressure distribution during the buffeting were, in general, of the type that would be associated with an angle-of-attack change.
2. In symmetrical pull-ups, at the beginning of the stall the greatest buffet intensity is located at the root of the tail surface but after the stall has developed spanwise on the wing the whole tail is enveloped by the buffet.
3. The average value of the increment in the tail normal-force coefficient due to buffeting was  $\pm 0.25$ .
4. The frequency of the pre-stall disturbances and those after the wing stall differ; both fluctuations appear regular enough to promote resonance if the tail were of the proper frequency.

Langley Memorial Aeronautical Laboratory  
National Advisory Committee for Aeronautics  
Langley Field, Va.

## REFERENCES

1. Rhode, Richard V.: Correlation of Flight Data on Limit Pressure Coefficients and Their Relation to High-Speed Burbling and Critical Tail Loads. NACA ACR L4I27, 1944.
2. Flight Research Maneuvers Section: Flight Studies of the Horizontal-Tail Loads Experienced by a Modern Pursuit Airplane in Abrupt Maneuvers. NACA ARR No. L4FO5, 1944.
3. Abdrashitov, G.: Tail Buffeting. NACA TM No. 1041, 1943.
4. Krzywoblocki, M. Zbigniew: Investigation of the Wing-Wake Frequency with Application of the Strouhal Number. Jour. Aero. Sci., vol. 12, No. 1, Jan. 1945.



## Airplane characteristics

### Wing

Area	236 sq.ft.
Span	37.29 ft.
MAC	6.8 ft.
Root chord	9 ft.
Section at root	NACA 2213
Section at tip	NACA 2209
Angle to thrust line	1 deg.
Dihedral	6 deg.
Aspect ratio	5.9

### Engine

Type	Allison V-1710-F4R
Normal power at 10800 ft.	1000 hp.
Propeller gear ratio	2:1
Propeller diameter	11 ft.

### Flight operation

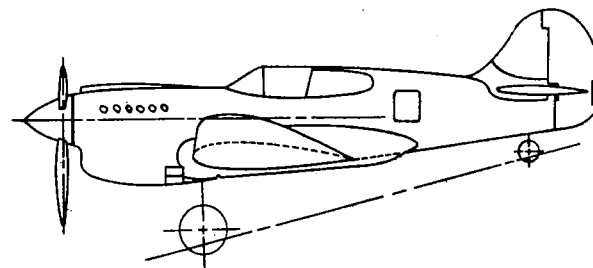
Average weight in flight	8200 lb.
Average C.G. position	29.5% MAC

### Vertical tail surface

Total area	22.9 sq.ft.
Height above fuselage	3.67 ft.
Fin area (less fairing area)	9.18 sq.ft.
Rudder area (including 1.94 sq.ft. of balance and .55 sq.ft. of tab)	13.74 sq.ft.
Distance from root L.E.W. to rudder hinge line	20.13 ft.
Fin offset	0 deg.
Fin extension	No. 1

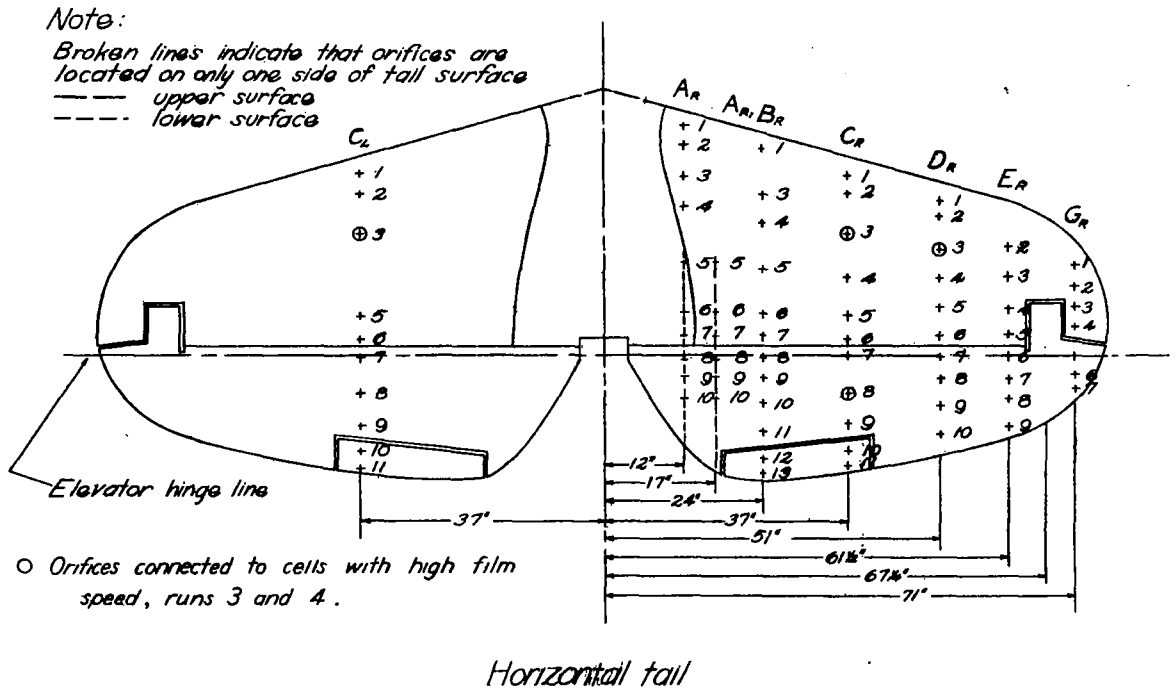
### Horizontal tail surface

Total area	48.3 sq.ft.
Span	12.79 ft.
Stabilizer area (including 3.54 sq.ft. of fuselage)	30.86 sq.ft.
Elevator area (including 3.8 sq.ft. of balance and 1.68 sq.ft. of tab)	17.44 sq.ft.
Distance from root L.E.W. to elevator hinge line	20.0 ft.
Stabilizer set above thrust line	2 deg.
Horizontal tail above fuselage center line	1.50 ft.
Max. elevator deflection	31.5° up



NATIONAL ADVISORY  
COMMITTEE FOR AERONAUTICS

Figure 1.- Three-view drawing and geometric characteristics of airplane used in tests (P-40K) .



Rib	Chord	Orifices*												
		1	2	3	4	5	6	7	8	9	10	11	12	13
A <sub>1</sub>	535	4.2	9.8	21.0	29.0	45.8	61.1	67.8	75.3	80.4	87.0			
A <sub>2</sub>	5125					40.1	54.5	61.1	67.6	72.9	79.0			
B <sub>1</sub>	565	4.4		17.7	25.6	38.9	51.7	57.9	62.8	69.9	77.5	85.8	93.0	97.4
C <sub>1</sub>	51.0	5.9	11.8	24.5	38.2	50.5	58.3	63.7	75.5	84.9	93.2	98.0		
D <sub>1</sub>	445	6.8	12.4	24.7	35.4	45.6	56.2	63.5	71.9	81.5	92.2			
E <sub>1</sub>	385		19.5	32.2	45.5	56.5	65.6	74.6	83.1	94.8				
G <sub>1</sub>	25.0	15.4	28.8	42.3	53.8		83.5	92.2						
C <sub>2</sub>	51.0	5.4	11.8	24.5		50.5	58.3	63.7	75.5	85.4	93.7	99.1		

\* Location in per cent chord from leading edge.

NATIONAL ADVISORY  
COMMITTEE FOR AERONAUTICS

Figure 2.-Location of orifices at which pressures were recorded.

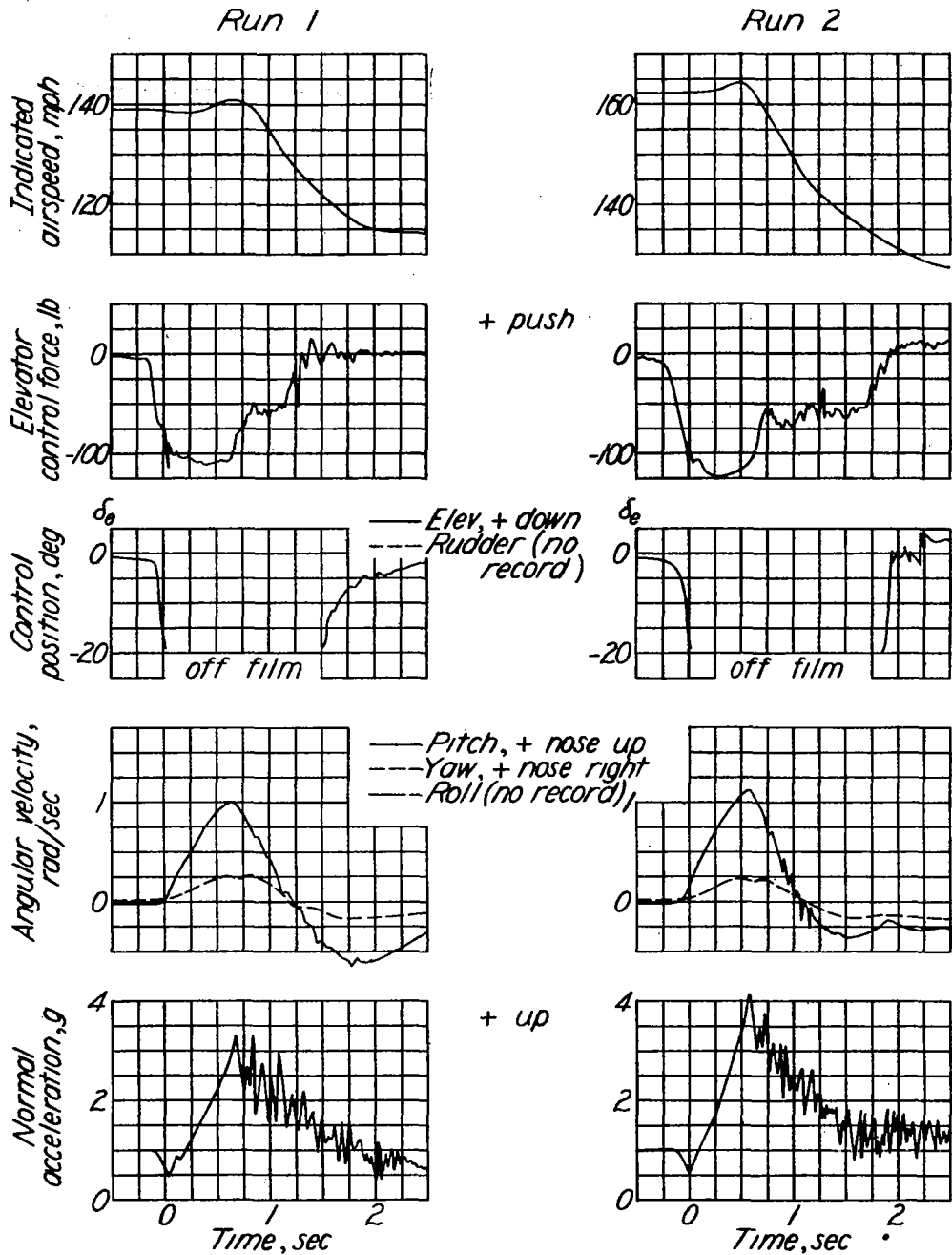


Figure 3.—Measurements from basic flight instruments during abrupt pull-ups to symmetrical stalls, Runs 1 and 2.

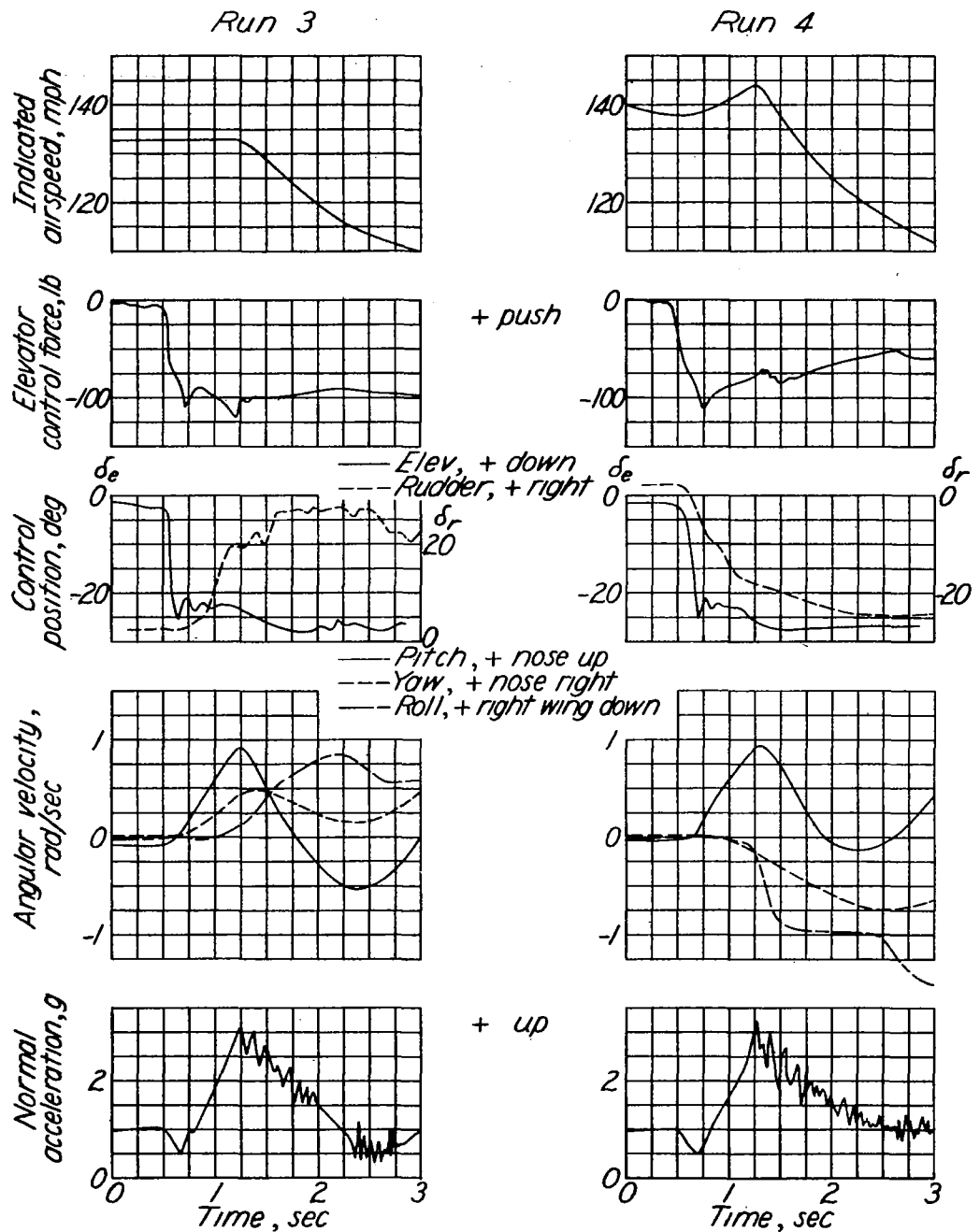


Figure 4.-Measurements from basic flight instruments during snap rolls to the right and to the left. Runs 3 and 4.

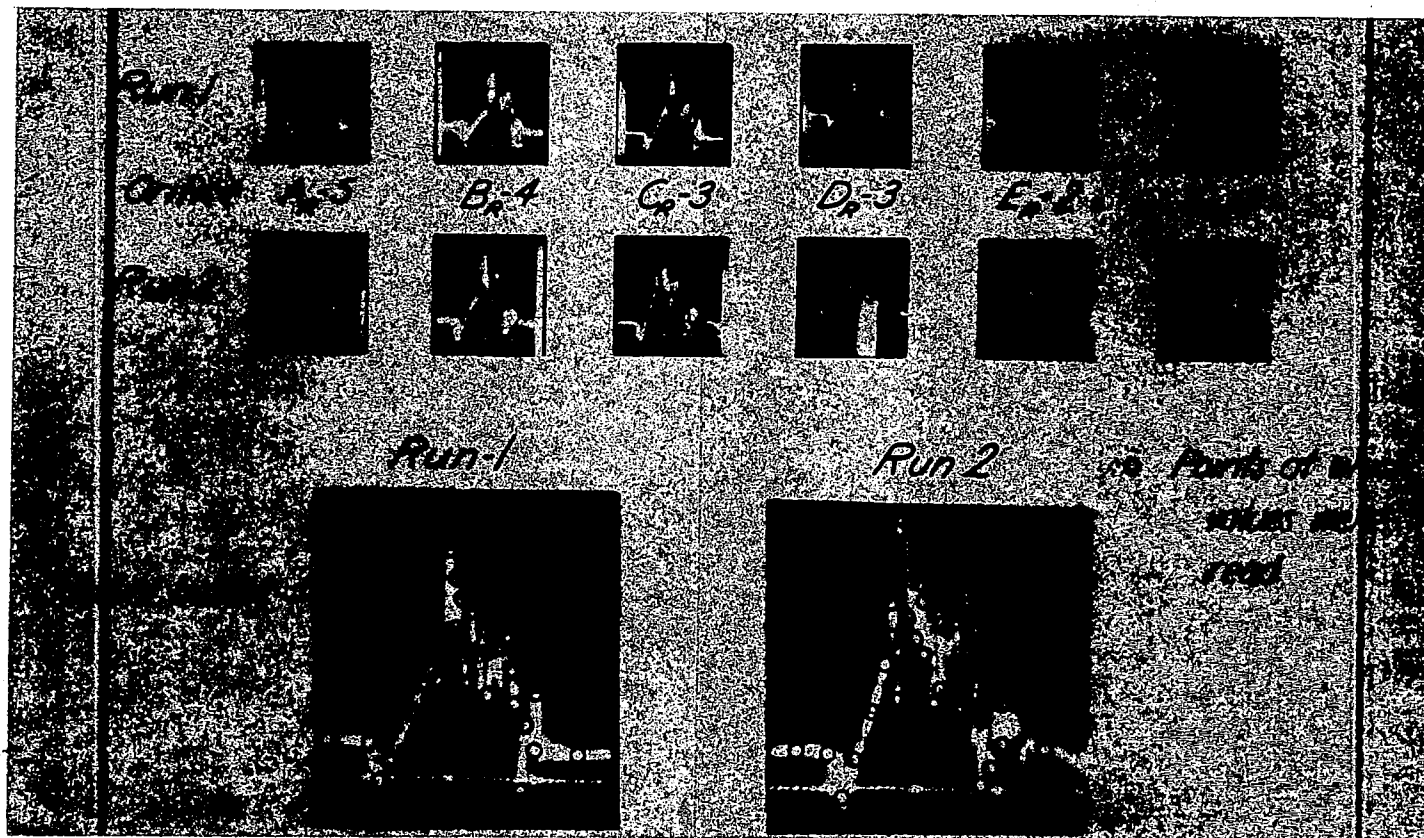
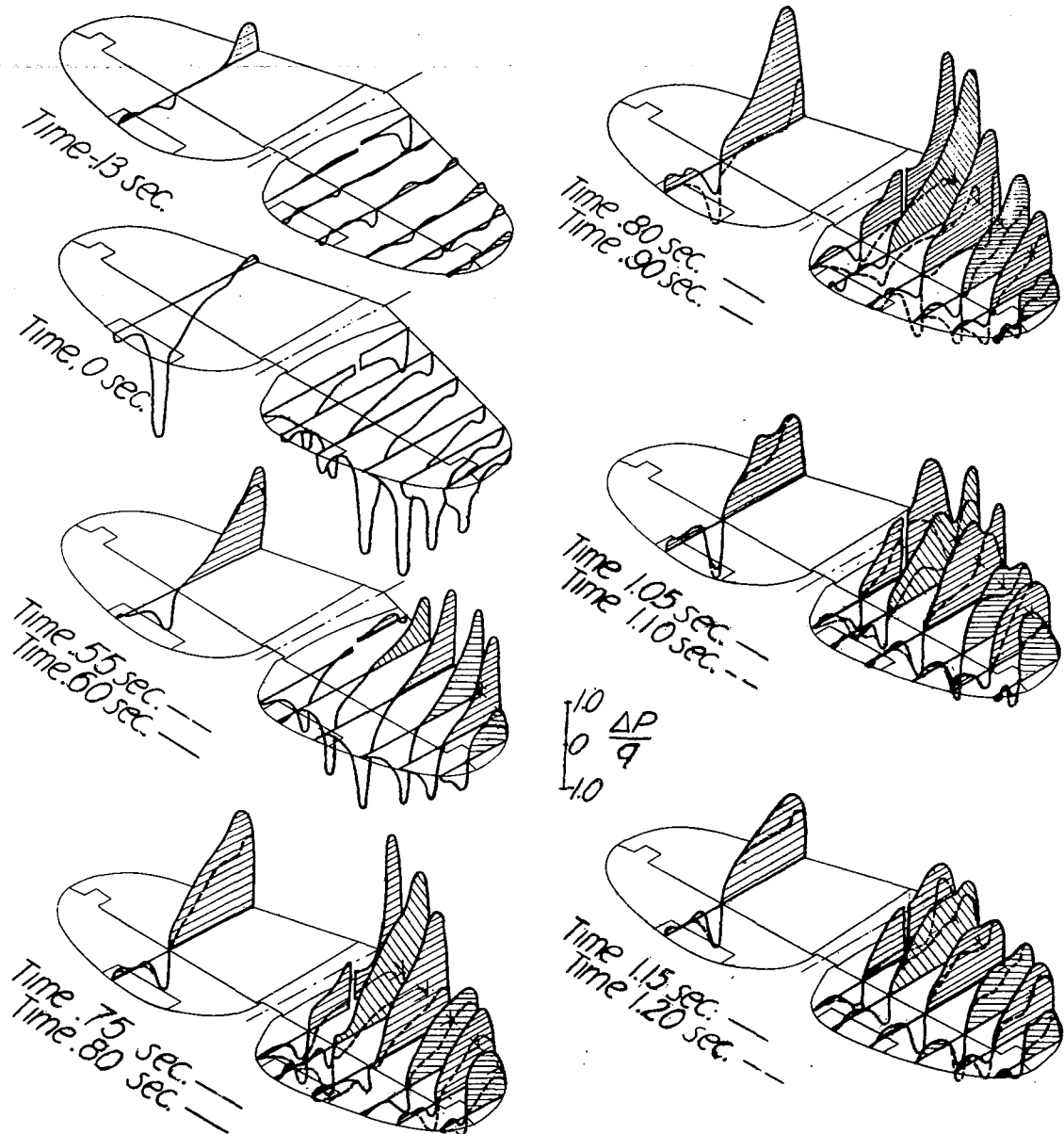


Figure 5.- Photographs of typical pressure records and enlargement showing time at which values were read for runs 1 and 2.



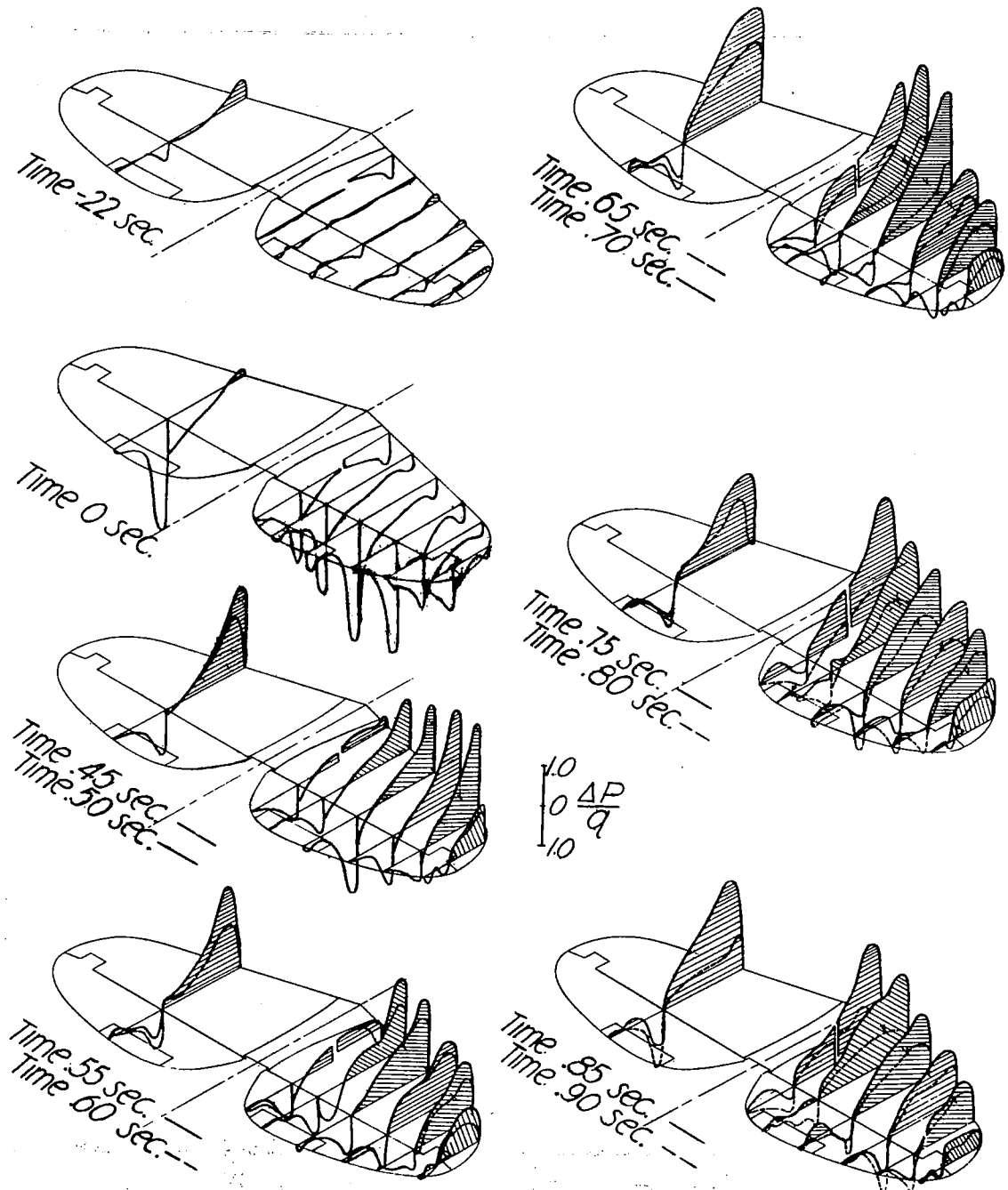
## Run 1



NATIONAL ADVISORY  
COMMITTEE FOR AERONAUTICS.

Figure 6. — Isometric views of pressure distributions during the abrupt stall pull-up of run 1.

## Run 2



NATIONAL ADVISORY  
COMMITTEE FOR AERONAUTICS.

Figure 7. — Isometric views of pressure distributions during the abrupt stall pull-up of run 2.

Rib  $C_L$

Rib  $A_R$

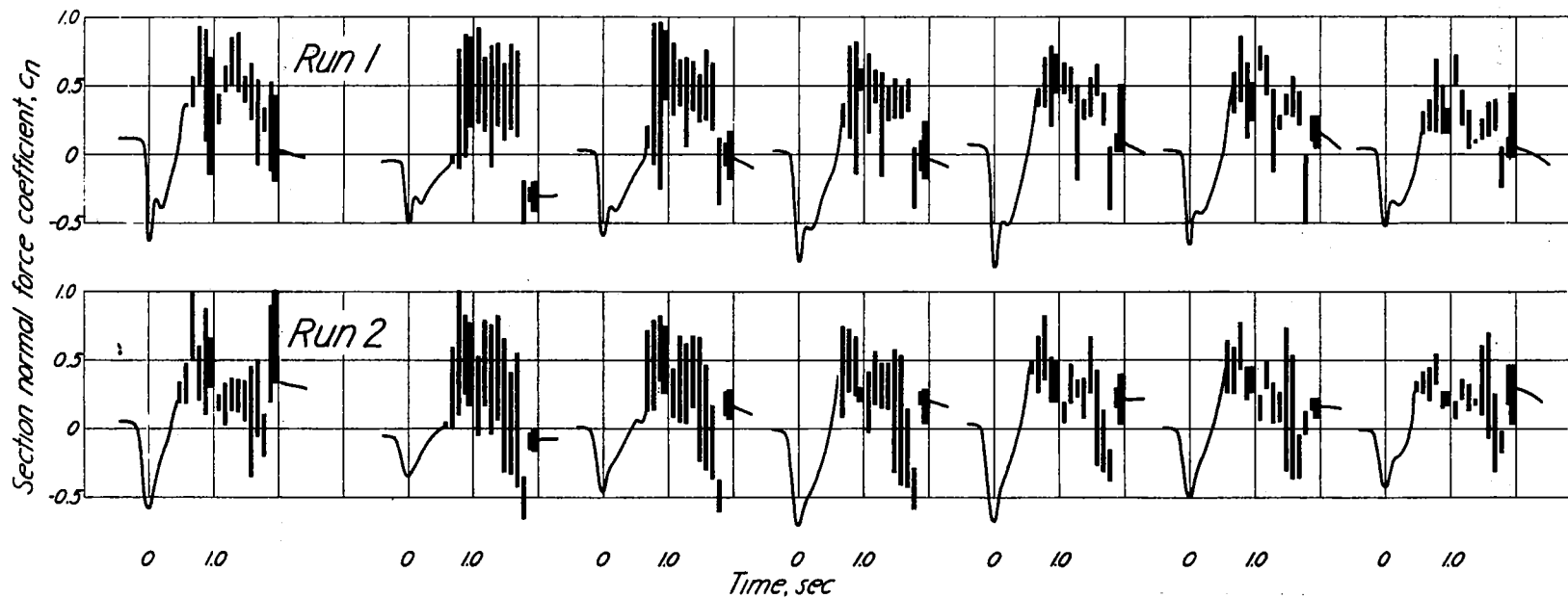
Rib  $B_R$

Rib  $C_R$

Rib  $D_R$

Rib  $E_R$

Rib  $G_R$



NATIONAL ADVISORY  
COMMITTEE FOR AERONAUTICS.

MR No. L5J06

Figure 8.-Variation of the rib normal force coefficients during the abrupt pull-ups of runs 1 and 2.

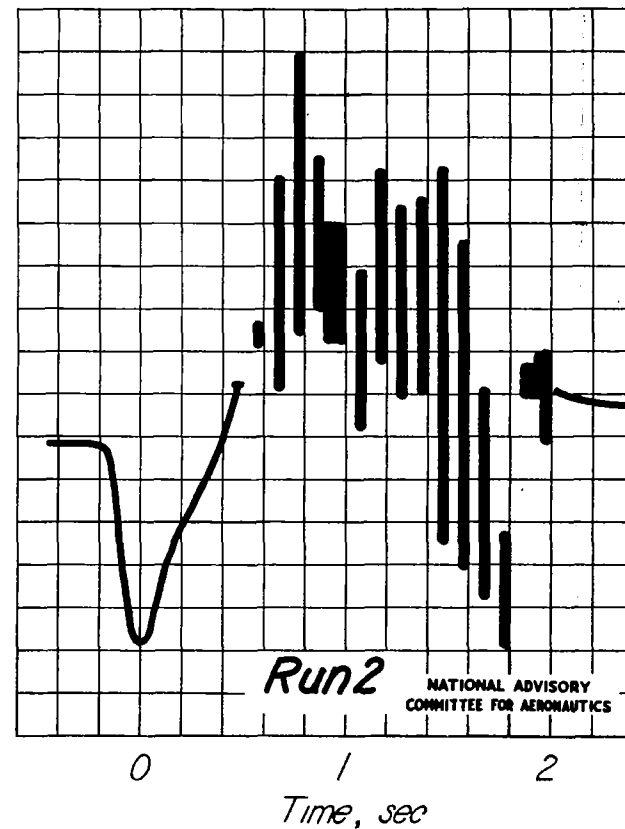
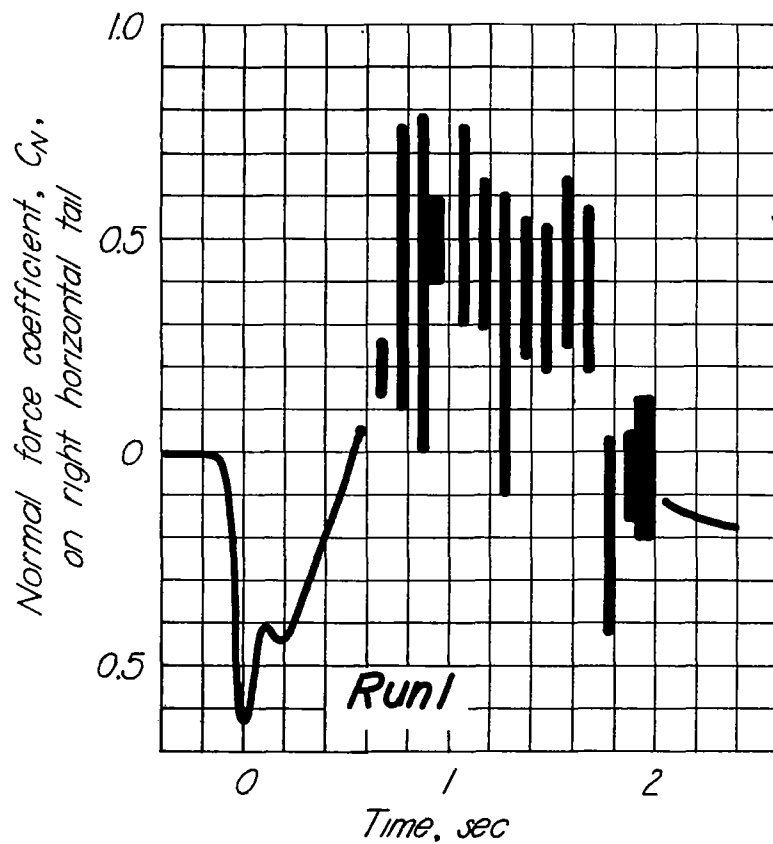


Figure 9. - Variation of normal force coefficient of right horizontal tail during stall pull-ups of runs 1 and 2

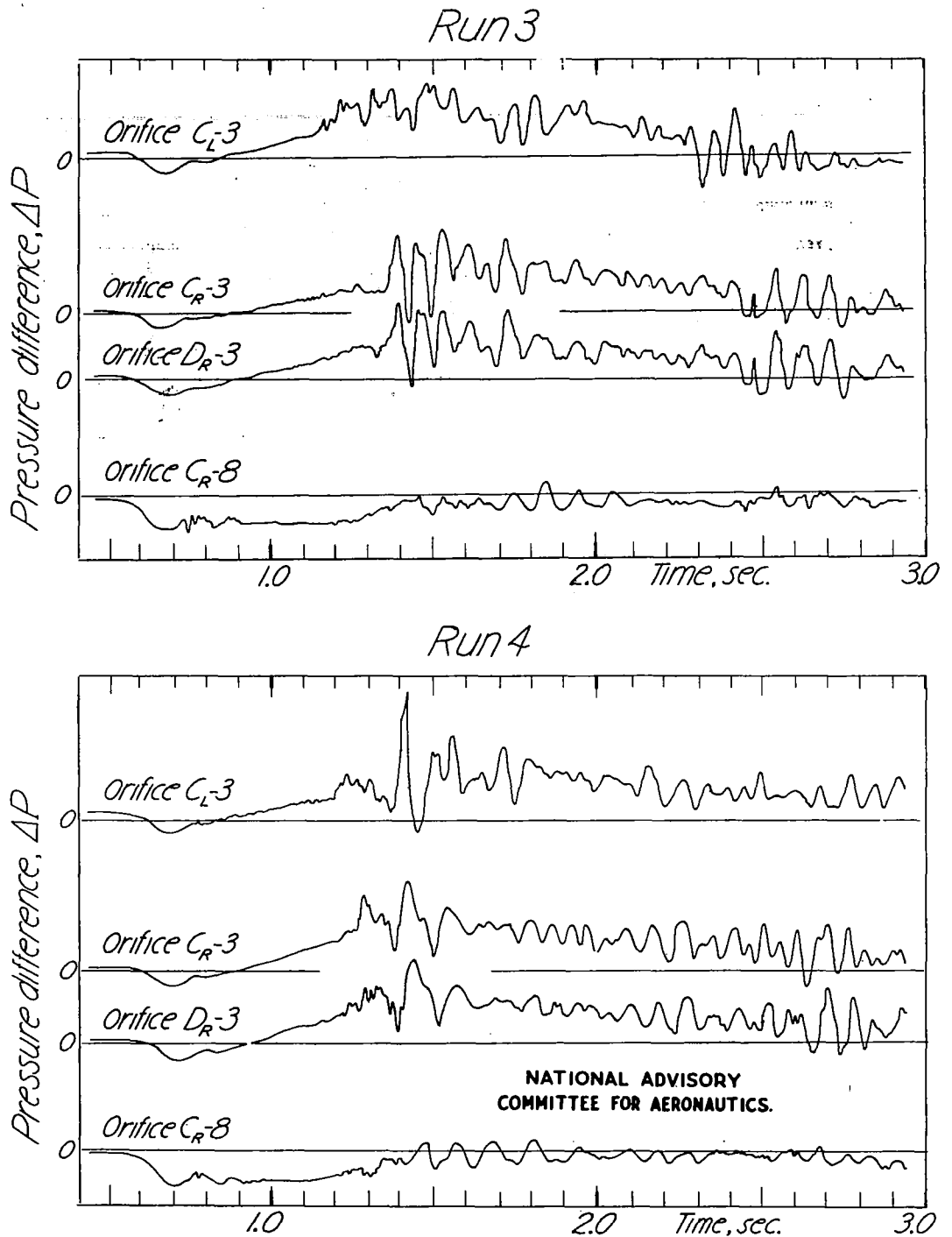


Figure 10.—Time history of pressures recorded during snap rolls to right and left, runs 3 and 4, respectively.

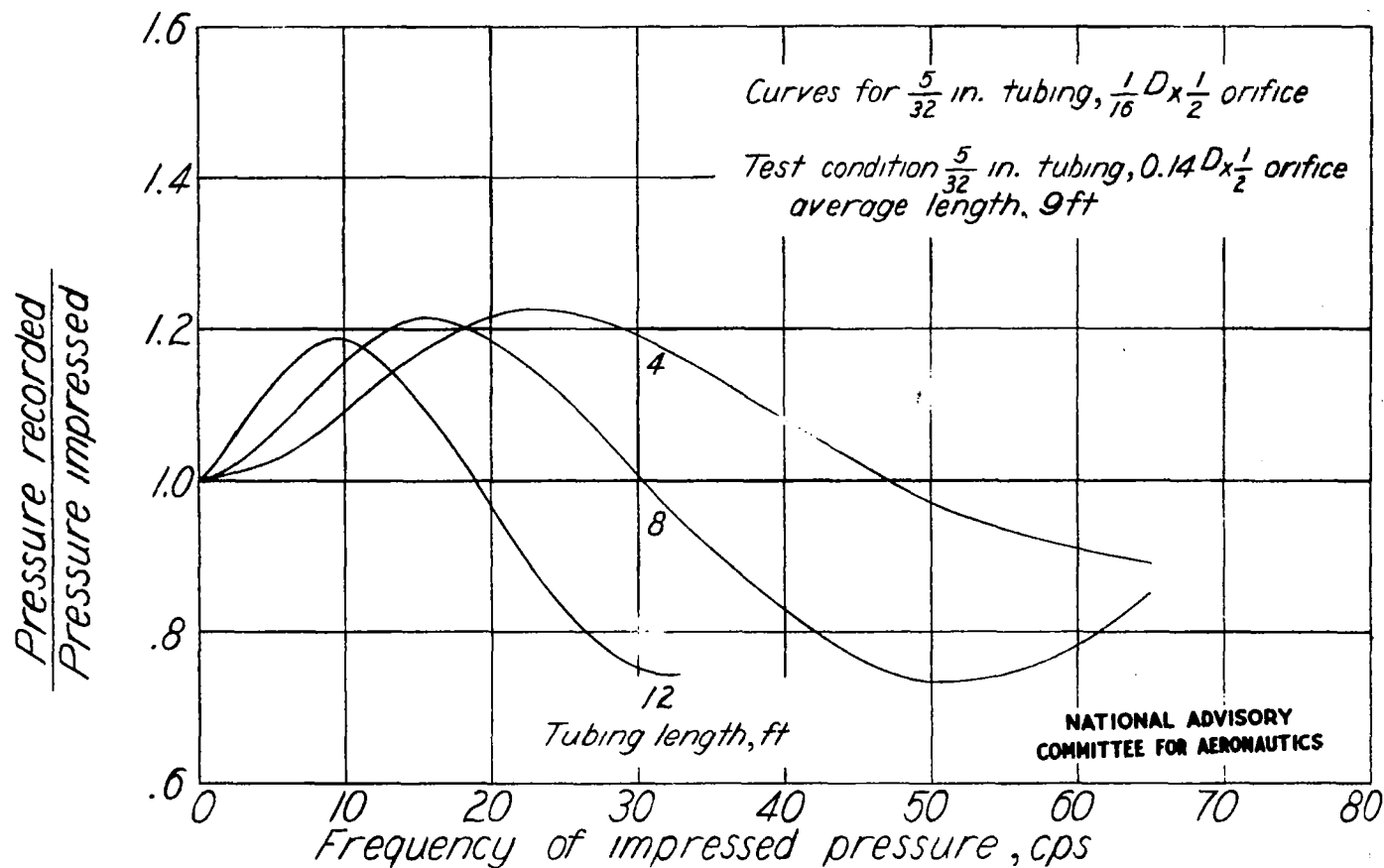


Figure 11.—Typical curves showing variation of pressure recorded with frequency of impressed sinusoidal pressure for tubing with orifices. (From unpublished test data)

NASA Technical Library



3 1176 01403 5399